

Synthesis, Characterization and Adsorption Study of C-4-Phenacyloxy-phenylcalix[4]resorcinarene for Pb(II), Cd(II) and Cr(III) Ions

(Sintesis, Pencirian dan Kajian Jerapan C-4-fenasiloksifenilkaliks[4]resorsinarena terhadap Pb(II), Cd(II) dan Cr(III))

UNDRI RASTUTI, DWI SISWANTA, WISNU PAMBUDI, BETA ACHROMI NUROHMAH, BOHARI M. YAMIN & JUMINA*

ABSTRACT

C-4-phenacyloxy phenyl calix[4]resorcinarene (CPPCR) was synthesized by acidic condensation of 4-hydroxybenzaldehyde and resorcinol. The adsorption of CPPCR for Pb(II), Cd(II) and Cr(III) has been studied by measuring the metal concentration in aqueous solution using Atomic Absorption Spectrophotometry (AAS). The effects of solution pH, contact time and initial concentration of metal ions on the adsorption capacity of CPPCR were investigated. The adsorption kinetic of all the ions obeyed the Ho and McKay pseudo 2nd order rate law and the adsorption isotherm profile matched very well with Langmuir model. The separation factor (R_L) of CPPCR for Pb(II), Cd(II) and Cr(III) were 0.190, 0.017, and 0.065, respectively, indicating the formation of monolayer behaviour. The Gibb free energy (ΔG) of the adsorption for all the metal ions have negative values indicating the adsorption process of Pb(II), Cd(II) and Cr(III) by CPPCR are spontaneous.

Keywords: Calix[4]resorsinarene; ion adsorption; isotherm adsorption; kinetics adsorption; 4-phenacyloxybenzaldehyde

ABSTRAK

C-4-fenasiloksifenilcalix[4]resorsinarena (CPPCR) telah disintesis melalui tindak balas berasid antara 4-hidroksilbenzalhid dan resorsinol. Penjerapan terhadap Pb(II), Cd(II) dan Cr(III) oleh CPPCR telah dikaji dengan mengukur kepekatan logam dalam larutan akueous menggunakan spektrofotometer serapan atom (AAS). Kesan pH larutan, masa sentuhan dan kepekatan awal ion logam ke atas kapasiti jerapan CPPCR telah dijalankan. Kinetik jerapan bagi semua ion logam tersebut mematuhi hukum pseudo-2nd Ho dan McKay serta profil isoterma jerapan pula menyetujui model Langmuir. Faktor pemisahan (R_L) bagi Pb(II), Cd(II) dan Cr(III) masing-masing adalah 0.190, 0.017 dan 0.065 yang menunjukkan berlaku tabii monolapisan. Nilai tenaga bebas Gibb bagi penjerapan semua logam bernilai negatif sekaligus menunjukkan proses yang spontan.

Kata kunci: Kaliks[4]resorsinarena; penjerapan ion; penjerapan isoterma; penjerapan kinetik; 4-fenasiloksibenzalhid

INTRODUCTION

Removal of organic waste and toxic metals contaminants from industrial activities are continuously being studied until now. It is a global problem as many countries are moving toward technological advancement and self-sustainability. The non-biodegradable nature and ecotoxicological and harmful effect on the human physiology of the metals are well established (Jaishankar et al. 2014). Lead, cadmium, chromium and other metals derived from mining industry waste, metal coatings, battery manufacture, chemical fertilizers, pharmaceuticals, electronics and textiles are toxic to animals and humans (Barnhart 1997; Flora et al. 2012; Satarug et al. 2003). Research on looking for new materials which are less toxic requires considerably a long time and removal or recycle the wastes is one popular strategy to overcome the problem. Among the conventional and unconventional methods of separating metal ions from the solution, adsorption was found to be effective, technically feasible and relatively low-cost in term of materials and process (Gunatilake 2015). Therefore, there have been a lot of studies on the adsorption technique especially looking for an effective absorbent.

Absorption of metal ions by activated carbon from different sources such as rice husk (Zhang et al. 2014), biomass (Joshi & Sahu 2014; Schneider et al. 2001), apricot stone (Abbas et al. 2014; Mouni et al. 2011) and method of treatment in order to get more active sites and large surface area have received much attention from the beginning until present. However, activated carbon from plants and animals based biomaterials are reported to having disadvantages such as high in cost and the used adsorbents may be considered as hazardous waste materials and also limited by less selectivity and probably caused agricultural problems (Reddy & Rao 2016).

The highest adsorption capacity achieved so far for lignin carbon against lead is 1865 mg g⁻¹ (Babel & Kurniawan 2003). The synthesized nano size carbon such as graphene oxide (GO) has impressive maximum adsorption capacities toward Pb(II) and Cd(II) up to 1119 and 530 mg g⁻¹, respectively (Sitko et al. 2013). However, it has been reported that it has a poor selectivity toward certain metals (Peng et al. 2017). The functionalized GO with silica (silica grafted GO) could increase the adsorption selectivity toward Pb(II) ions to reach over

99% in the presence of others metal ions (Li et al. 2015). Montmorillonite clay has been reported to have adsorption capacity toward Pb(II) and Cd(II) around 33.0 and 32.7 mg g⁻¹ (without treatment) and its capacity increased to 34.0 and 33.2 mg g⁻¹ after acid-activation (Bhattacharyya & Gupta 2008; Gupta & Bhattacharyya 2009).

Agro-based industrial waste is another potential absorbent which is plentiful and cheap. Indonesia and Malaysia are the world major producers of palm oil. The amount of empty fruit bunch (EFB) fiber by-products from the oil-palm industry is huge. The presence of hydroxyl groups in the EFB enables it to be modified to enhance the adsorption capacity. Modification via grafting of carboxylic and amines groups on the EFB backbone has shown good adsorption capability for the removal of an organic dye such as methylene blue (Sajab et al. 2013). In addition, it has also demonstrated an increase in adsorption capacity for metal ions such as Cu(II), Ni(II), Mo(VI) and As(V) in aqueous solution in both single and binary systems. The adsorption behavior fitted quite well with the kinetic-interparticle diffusion and both Langmuir and Freundlich isotherm models (Sajab et al. 2017).

Biopolymers, such as chitosan, alginate, cellulose and keratin are naturally biodegradable and non-toxic materials (Tran et al. 2016). Despite their great abundance in nature, each of them requires further treatment or process into a usable form such as films and fibers which may become less cost-effective (Mututuvvari 2014). In 2011, Benavente et al. (2011) reported the adsorption capacity of chitosan from shrimp shell waste for Cu(II), Hg(II), Pb(II) and Zn(II) were 79.94, 109.55, 58.71 and 47.15 mg g⁻¹, respectively. A recent study reported the adsorption capacity of chitosan were 10 and 41.4 mg g⁻¹ against Cd(II) and Cr(VI), while modification to chitosan-activated carbon composite significantly increases the capacity up to 52.63 and 90.9 mg g⁻¹, respectively (Shariffard et al. 2016).

Among the synthetic absorbents, calixarene has a unique cup-like structure which may capture natural molecules or ions or provide host-guest interaction leading to adsorption. In addition, it is a macrocyclic oligophenols not only providing active sites but also chemical modifications through the hydroxyl groups. A number of calix[4]arenes have been reported as potential absorbents for heavy-metal ions (Akkus et al. 2009; Kunsagi-Mate et al. 2005). A larger macrocyclic calix[6]-Na-hexasulphonate also displayed similar activity. Twenty four adsorption of dye waste by calix[n]arene was also reported (Ming et al. 2011). Calix[n]resorcinarene has benzene derivatives groups as the linkers connecting the diphenol groups and offers wide functionalization to modify the structure that might be tailored to the desired adsorption capability.

C-4-hydroxyphenylcalix[4]resorcinarene has shown adsorption capability for Mn(II), Cu(II), Co(II), Zn(II) and Pb(II) ions (Trawneh 2015). The study of adsorption characteristics of Pb(II) and Cr(III) ions onto C-4-methoxyphenylcalix[4]resorcinarene (CMPCR) in batch and fixed bed column systems has been conducted

(Jumina et al. 2007). In their studies, the adsorption kinetic of Pb(II) and Cr(III) adsorptions followed pseudo 2nd order kinetics model. The R_L value also shows that the adsorption of Pb(II) (R_L=0.145) was more favorable than Cr(III) (R_L=0.372). The adsorption capacity of Pb(II) was 4.166 mg g⁻¹ in the column system which is much higher than from batch system with only 0.85 mg g⁻¹. Similar result was also shown by CMPCR toward Cr(III) with adsorption capacity of 0.895 and 0.61 mg g⁻¹ for column and batch system, respectively. The adsorption properties of C-methylcalix[4]resorcinarene (CMCR) prepared by one-step reaction of resorcinol and acetaldehyde and HCl was reported (Jumina et al. 2011). The adsorption capacity of CMCR for Cr(III) and Pb(II) was found to be 3.644 mg g⁻¹ (70.07 μmol g⁻¹) and for was 9.201 mg g⁻¹ (44.45 μmol g⁻¹), respectively.

In continuing our work on the adsorption of calix[4]resorcinarene, a new 4-phenacyloxyphenylcalix[4]resorcinarene (CPPCR) containing both carbonyl and hydroxyl groups active sites was synthesized via the condensation reaction of 4-phenacyloxybenzaldehyde and resorcinol (Figure 1). The adsorption study of CPPCR for Pb(II), Cd(II) and Cr(III) are reported.

EXPERIMENTAL DETAILS

MATERIALS AND METHODS

All reagents and solvents were purchased from either E. Merck Inc. or Sigma-Aldrich and used without further purification. Reagents used in this research include resorcinol, hydrochloric acid (HCl), methanol, Pb(II), Cd(II) and Cr(III) standard solution (1000 ppm); and aqua-bidest. Intermediate compound 4-phenacyloxybenzaldehyde (PB1) was synthesized according to Rastuti et al. (2016).

INSTRUMENTATIONS

NMR spectra were recorded using NMR Spectrophotometer, JOEL ECZ 500 M (¹H-NMR 500 Hz; ¹³C-NMR 125 Hz). Mass spectra were acquired with High-Resolution Mass Spectrophotometer, HRMS ESI-TOF, LCT Premier XE. IR spectra were recorded with an FTIR, Shimadzu Prestige 21. Melting point was determined using Electrothermal 9100. The concentration of ions was determined using an Atomic Absorption Spectrophotometer (AAS, AA-6650F Shimadzu).

GENERAL PROCEDURE

Synthesis of C-4-Phenacyloxy Phenylcalix[4]Resorcinarene (CPPCR) CPPCR was synthesized based on Gutsche's method (Gutsche 2008) with slight modification. A mixture containing resorcinol (0.50 g, 5 mmol), 4-phenacyloxybenzaldehyde (1.2 g, 5 mmol) and concentrated HCl (0.50 mL) in methanol (50 mL) was refluxed at 65°C for 24 h. The reaction mixture was cooled to reach room temperature and added with water (50 mL). The precipitate formed

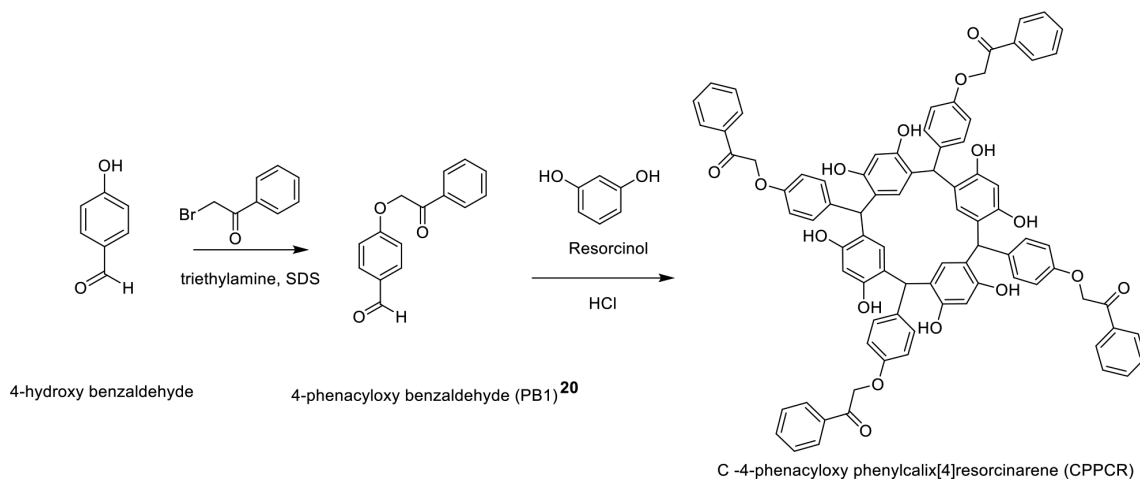


FIGURE 1. Synthesis of 4-phenacyloxy phenyl calix[4]resorcinarene (CPPCR)

was then filtered, washed using methanol: water (1:1), neutralized with water and dried in a desiccator (silica gel) to get brown solid in a yield of 75.90%; m.p. 288°C (dec.); FT-IR (KBr) (cm^{-1}): 3387 (OH phenol), 3070 (CH aromatics), 2978 (CH aliphatic), 1689 (C=O ketone), 1604–1504 (C=C aromatics), 1442 (–CH– bending), 1226–1080 (COC ether). $^1\text{H-NMR}$ (δ ppm, acetone- d_6 , 500 MHz): 8.00 (4H, s, –OH); 6.18–7.51 (22H, m, aromatic proton); 5.70 (4H, s, methylene – CH_2 –); and 5.39 (2H, s, –CH–). $^{13}\text{C-NMR}$ (δ ppm, acetone- d_6 , 125 MHz): 195.32 (C=O), 154.27 and 158.22 (aromatic carbon adjacent to oxygen ether and alcohol), 115.21–135.90 (aromatic carbons), 42.36 (methylene carbon – CH_2 –). HRMS: m/z $\text{M}+\text{Na}^+$ = 1351.49.

General Experimental Protocol The batch adsorption experiments were conducted in a set of 10 mL sized flask containing CPPCR adsorbent and metal solutions in various initial concentrations. The pH of the solution was adjusted with 0.01 M HCl and 0.01 M NaOH prior to the adsorption experiments. The bottles were agitated in an isothermal water-bath shaker at room temperature until the equilibrium is reached. The solution was then filtered and the concentration of the residual metal ions in the solutions was determined by measuring their absorbance using AAS spectrophotometer. The uptake amount of metal ion was calculated by subtracting the initial concentration with the concentration after adsorption process. The adsorbed quantity and percentage removal of metal ions were calculated using the following equations:

$$q_e = (C_o - C_e) \times \frac{V}{M} \quad (1)$$

$$q_t = (C_o - C_t) \times \frac{V}{M} \quad (2)$$

and

$$\% \text{ removal} = \frac{(C_o - C_t)}{C_o} \times 100\% \quad (3)$$

where q^e is the adsorption capacity at equilibrium (mg/g); q^t is the adsorption capacity of adsorbent for metal ions at time t , t (mg/g); C_o is the initial metal ion concentration in the aqueous phase (mg/L); C_e is the equilibrium metal ion concentration in the aqueous phase (mg/L); C_t is the concentration of metal ions at time t (mg/L); V is the volume of the solution used (mL); and M is the mass of the adsorbent used (mg).

Adsorption Profile Experiments Similar procedure as described in the general protocol was followed in the studies of adsorption profile. A set of seven flasks of a solution containing 10 mL of 10 ppm metal ions (Pb(II), Cd(II) and Cr(III)) with adjusted pH at 4, 6 and 4.5 were prepared, respectively. CPPCR adsorbent (0.01 g) was then added to each of the solution set. In addition, each flask was paired with exactly similar solution sample except for the existence of the adsorbent as a blank or control for the determination of metal concentration by AAS spectrometer. The solutions were then agitated at room temperature for seven different contact times of 5, 15, 30, 60, 120, 180 and 240 min. At each contact time, the solution was quickly filtered and measured their absorption by using the AAS together with its blank solution. Adsorption profile was determined based on the following equation:

Lagergren equation:

$$\log(q_e - q_t) = \log q_e - \frac{k}{2.303} t \quad (4)$$

Ho and McKay equation:

$$\frac{t}{q_t} = \frac{1}{kq_e^2} + \frac{1}{q_e} t \quad (5)$$

Santosa equation :

$$\frac{\ln(C_o / C_t)}{C_t} = \frac{k}{C_i} t + k \quad (6)$$

where q_e amount of metal ions absorbed at equilibrium (mg/g); q_t is the amount of metal ions absorbed at time t (mg/g); k is the rate constant of adsorption (min^{-1}); t is the contact time (min); C_o is the initial concentration of metal ions in the aqueous phase (mg/L); and C_t is the concentration of metal ions at time t (mg/L).

Effect of Solution pH Optimum pH is described as the pH values that give the highest adsorption uptake (%) of metal ions. In this study, determination of optimum pH was carried out by measuring the CPPCR adsorption to the Pb(II), Cd(II) and Cr(III) metal ions at various pH values. A series of metal ions solution (10 ppm) was prepared, respectively and it consisted of six solutions with pH of 2, 3, 4, 5, 6 and 7. Into the solution sample was added with as much as 0.01 g adsorbent (CPPCR). Each solution has its own blank which was similar to the sample solution without addition of CPPCR adsorbent. Both series of sample and blank solutions were stirred for 3 h at room temperature and the solid adsorbent was then filtrated. The concentration of metal ions in the sample and blank solutions were determined by measuring their absorbance using AAS spectrometry. The amount of adsorbed metal ion was calculated by subtracting the initial concentration (blank solution) with the concentration after adsorption process.

Effect of Adsorbent Dosage Optimization of the initial concentration of Pb(II), Cd(II) or Cr(III) ions was conducted by varying the initial concentration of metal ions (0, 4, 8, 12, 16, 20 ppm) and 0 ppm was ascribed as a blank solution. A 0.01 g of CPPCR was added into 10 mL of each metal ion solution at the optimum pH. The mixture was then stirred for a corresponding time (optimum time) at room temperature. The solid CPPCR was filtered and the concentration of metal ions in the filtrate was determined by measuring their absorbance using AAS spectrometry. The amount of metal cation adsorbed was determined from the different metal ions concentration in the solution before and after adsorption process.

Three adsorption isotherm equations, Langmuir, Freundlich and Temkin were used to determine the adsorption isotherm and displayed as follow:

Langmuir equation:

$$\frac{1}{q_e} = \frac{1}{K_L q_m C_e} + \frac{1}{q_m} \quad (7)$$

$$\frac{C_e}{q_e} = \frac{1}{K_L q_m} + \frac{C_e}{q_m} \quad (8)$$

where C_e is the equilibrium concentration of metal ion (mg/L); q_e is the amount of metal adsorbed per gram of the adsorbent at equilibrium (mg/g); q_m is the maximum monolayer coverage capacity (mg/g); and K_L is the Langmuir isotherm constant (L/mg).

Freundlich equation:

$$\log(q_e) = \log(KF) + \frac{1}{n} \log(C_e) \quad (9)$$

where K_F is the Freundlich isotherm constant (mg/g); n is the adsorption intensity; C_e is the equilibrium concentration of adsorbate (mg/L); and q_e is the amount of metal adsorbed per gram of the adsorbent at equilibrium (mg/g).

Temkin equation:

$$q_e = B \ln A_T + B \ln C_e \quad (10)$$

where B is $\frac{RT}{b}$; A_T is Temkin isotherm equilibrium binding constant (L/g); b_T is the Temkin constant; and R is the universal gas constant (8.314 J/mol/K).

RESULTS AND DISCUSSION

SYNTHESIS OF C-4-PHENACYLOXY PHENYL CALIX[4] RESORCINARENE (CPPCR)

C-4-phenacyloxy phenyl calix[4]resorcinarene (CPPCR) was obtained as a solid powder with a yield of 75.9%. No melting point was observed but it began to decompose at about 288°C. The FTIR spectrum showed the disappearance of an aldehyde absorption band at 1689 cm^{-1} (Figure 2(b)) and the presence of distinct broad absorption band at 3387 cm^{-1} due to the hydroxyl groups (-OH) stretching from the resorcinol.

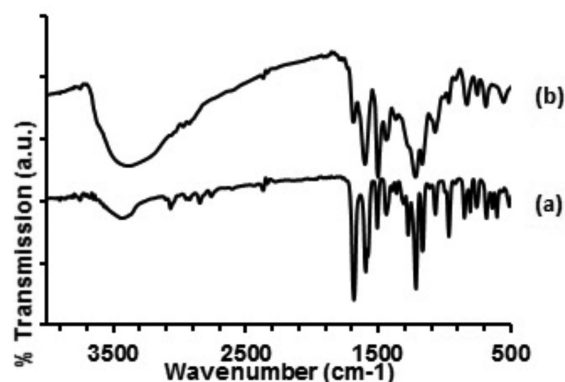


FIGURE 2. (a) IR spectrum of 4-phenacyloxy benzaldehyde and (b) 4-phenacyloxyphenylcalix[4]resorcinarene (CPPCR)

The $^1\text{H-NMR}$ spectrum (Figure 3) showed a rather complex splitting pattern that make an assignment work a bit difficult with 12 benzene rings and the possibility of several conformations exists in the solution. However, it is still possible to locate the chemical shift range for the protons (Figure 3). Generally, hydrogen bonded aromatic hydroxyl protons appear down field and in this case at δ 8.0 ppm with singlet appearance marked as a. The proton d at δ 5.39 ppm indicates the methine bridge. The proton

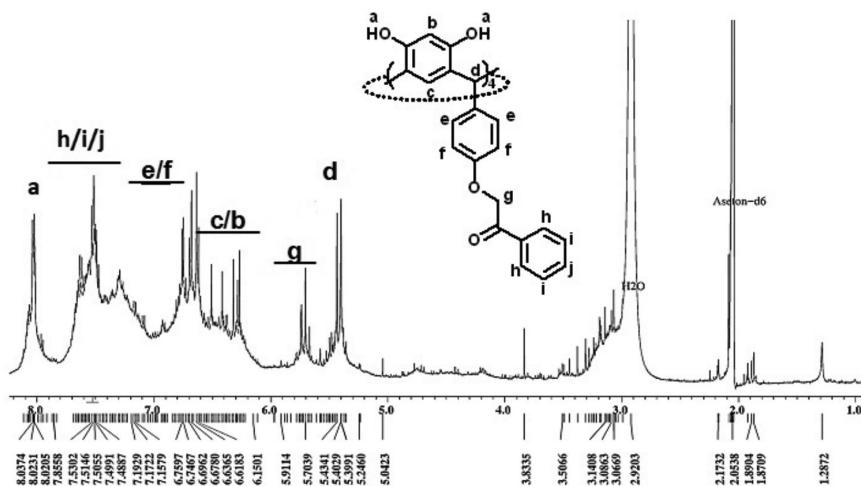


FIGURE 3. ^1H -NMR spectrum of 4-phenacyloxy phenyl calix[4]resorcinarene (CPPCR) in d_6 -acetone

g at δ 5.70 shift shows the methylene proton ($-\text{CH}_2-$) in the phenacyl group. Protons b and c at δ 6.18-6.67 ppm show aromatic protons on the resorcinol benzene. Protons e and f at δ 6.69 and 7.15 ppm, respectively are the protons of the phenyl aromatic rings. Chemical shift i, j and h in the range of δ 7.49-7.51 show protons in the phenacyl group. The fact that the total number of protons calculated from the nmr integration is half of the actual number indicates that the molecule is symmetrically generated. The ^{13}C -NMR spectrum (Figure 4) showed carbon of carbonyl group (C1) appears at δ 195 ppm. Carbon of methine bridge (C15) is shown at δ 15 ppm. Methylene carbon (C14) appears at δ 42 ppm. All the carbons on the aromatic ring of resorcinol, the benzene and the phenacyl group (C2-C13) appear at δ 46-158 ppm. The high-resolution mass spectrometry (HRMS) spectrum (Figure 5) further confirm the formation of cyclotetramer structure of CPPCR as shown by the presence of molecular ion peak at m/z 1352 ($\text{M}+\text{Na}^+$) which is the molecular weight of CPPCR.

ADSORPTION STUDY OF CPPCR

Adsorption Profile The absorption profile of CPPCR against Pb(II), Cd(II) and Cr(III) was obtained by measuring the adsorption of the metal ions at different contact times 5, 15, 30, 60, 120, 180, and 240 min. Plots of adsorption ($C_0 - C_t$) against time for all the metals showed an increase in the quantity of metal ions adsorbed as the contact time increases until it reaches an equilibrium time at 60, 120 and 120 min for Pb(II), Cd(II) and Cr(III), respectively. This pattern was followed by a slow decrease after the equilibrium times indicating a desorption step (Figure 6). The adsorption of Cr(III) was somewhat peculiar with spontaneous adsorption to reach equilibrium within 10 min followed by a decrease in adsorption before increasing again. A similar pattern was observed in the previous adsorption studies of CMPCR for Cr(III). In fact, the increase was almost verticle before reaching a steady value which took about 5 min (Jumina et al. 2007). In the present work, the adsorption of Cd(II) reached equilibrium quite rapidly and became steady within 10 min. The adsorption of Pb(II)

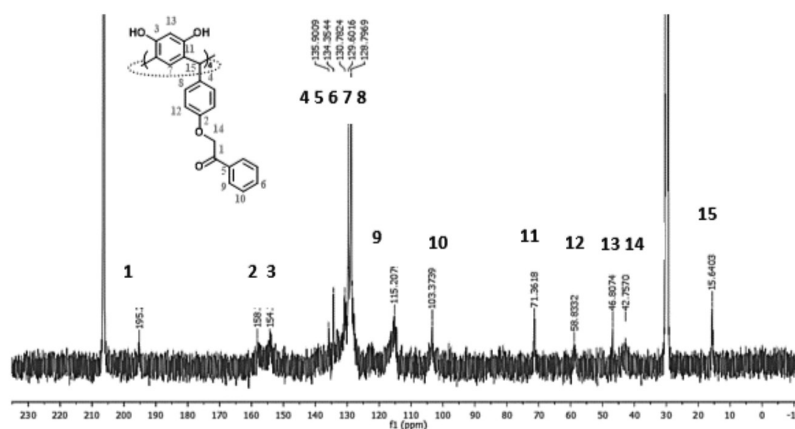


FIGURE 4. ^{13}C -NMR spectrum of 4-phenacyloxy phenyl calix[4]resorcinarene (CPPCR) in d_6 -acetone

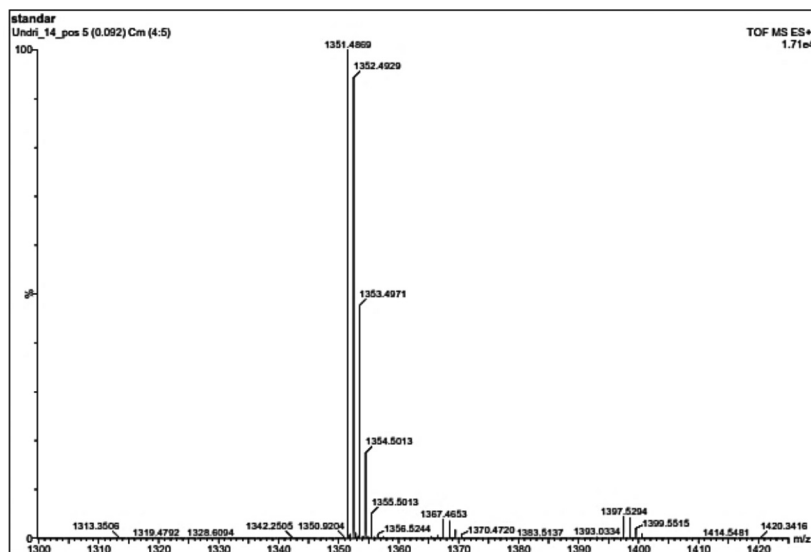
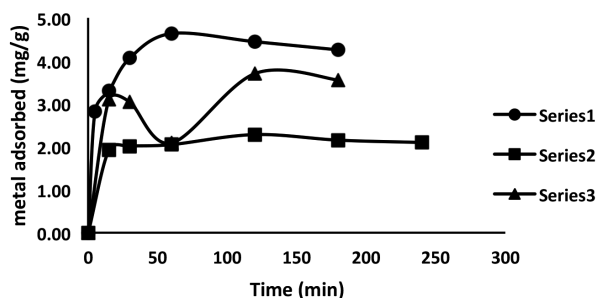


FIGURE 5. HRMS spectrum of 4-phenacyloxy phenyl calix[4]resorcinarene (CPPCR)

showed a typical relatively slow increase approaching the equilibrium maxima within an hour and followed by a slow decrease (Figure 6).



$[Pb]_0 = 10 \text{ mg/L}$, $[Cd]_0 = 2.5 \text{ mg/L}$, $[Cr]_0 = 20 \text{ mg/L}$ and $[CPPCR] = 0.01 \text{ g}$

FIGURE 6. Adsorption of Pb, Cd, and Cr by CPPCR in aqueous solution

The plots of adsorbed Pb(II), Cd(II) and Cr(III) metals (q_t) and percentage removal against time showed the typical adsorption behavior on the active surface (Figures 6 & 7). It was also realized that the maximum adsorption of chromium and cadmium were lower compared to lead. Adsorption capacity of CPPCR toward Pb(II), Cd(II) and Cr(III) at equilibrium state were 4.63, 2.28 and 3.70 mg g^{-1} , respectively, (Pb(II) > Cr(III) > Cd(II)). Meanwhile, it gave different order based on the maximum percentage of removal i.e. Cd(II) > (Pb(II) > Cr(III) with 95.5, 55.8 and 19.4%, respectively. Therefore, it may not be possible to analyze the data in detailed for Cr(III).

As a preliminary study, the UV-Vis spectrum of Cr(III) (NO_3)₃ solution in the presence of the adsorbent was recorded for 2.5 h at 5 min interval and the result could give some information regarding what happened in the solution. Pb(II) and Cd(II) solutions do not show uv-vis peak for

the same study. Under low concentrations no significant peak shift of Cd ($\lambda_{\text{max}} = 577, 410$ and 300 nm) after the addition of calix was observed. The decrease of absorbance at all wavelengths was very low, only about 0.4% of Cr was absorbed even after 24 h of contact time (Figure 8). The observation seems to be in agreement with the result obtained by Atomic Absorption Spectrophotometer (AAS) measurement. Further study by varying the concentration of adsorbant-adsorbate will certainly give more information about the adsorption behaviour.

Adsorption Kinetics Kinetic order and the adsorption parameters were analyzed by applying the Santosa and Lagergren 1st order kinetic and also Ho-MacKay pseudo 2nd order models. The correlation coefficient (R^2) was determined from a linear plot of $\ln(C_0/C_t)/C_t$ vs t/C_t ; $\log(q_e - q_t)$ vs t and t/qt vs t . Table 1 shows the kinetic modeling for CPPCR against Pb(II), Cd(II) and Cr(III). Based on the result, it appeared that the Ho-MacKay pseudo 2nd order was the best kinetic modeling of CPPCR. The plots of the pseudo 2nd order showed a good straight line (Figure 9) with a good R^2 value. This result was similar to the previous study of C-4-methoxyphenylcalix[4]resorcinarene (CMPCR) and C-methylcalix[4]resorcinarene (CMCR) as an adsorbent for Pb(II) and Cr(III), that also follow the Ho-MacKay pseudo 2nd order model (Jumina et al. 2011, 2007). Trawneh et al. (2015) also investigated the adsorption kinetics of C-4-hydroxyphenylcalix[4]resorcinarene against Cu(II), Co(II), Zn(II), Mn(II), and Pb(II) metal ions and the kinetic also follow the pseudo 2nd order kinetic model.

Based on the 2nd order rate constants (k), the adsorption rate of Cd(II) ($1.423 \text{ g mg}^{-1} \text{ min}^{-1}$) was about 10 fold times higher than Pb(II) ($0.135 \text{ g mg}^{-1} \text{ min}^{-1}$) and almost 100 times of Cr(III) ($0.016 \text{ g mg}^{-1} \text{ min}^{-1}$). This result implied that the adsorption of CPPCR toward Cd(II) ions was the fastest although its adsorption capacity (q_e)

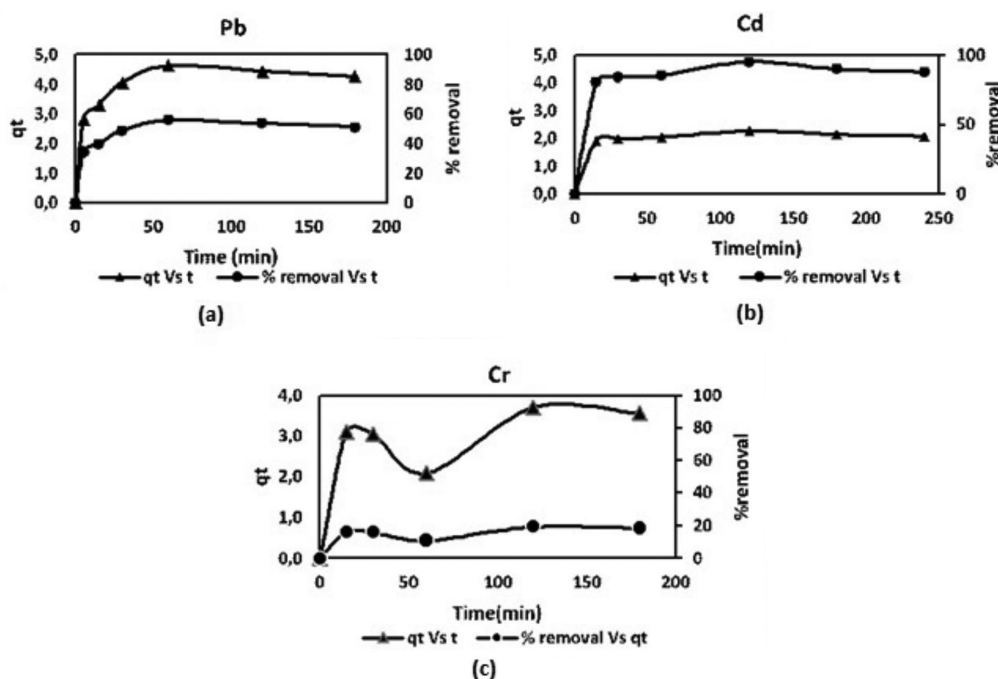


FIGURE 7. Adsorption and %removal against time plot for (a) Pb(II) (b) Cd(II) and (c) Cr(III)

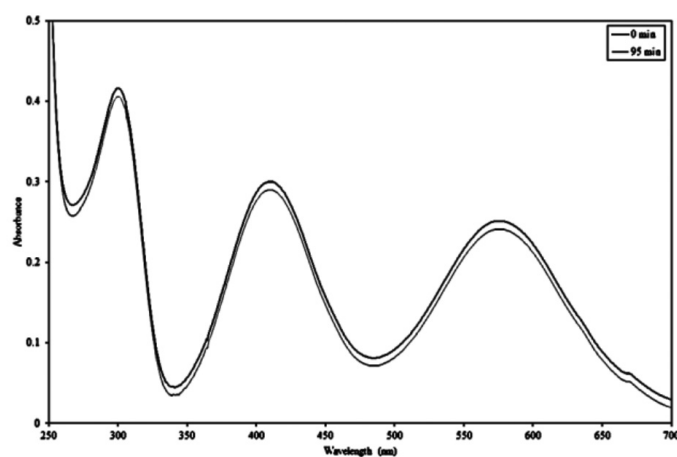


FIGURE 8. The spectrum of chromium nitrate solution in the presence of CPPCR recorded immediately (top spectrum) and after 95 min. $[CPPCR]_0 = 0.01$ g; $[Cr(III)]_0 = 20$ mg/L; $T = 26^\circ C$

TABLE 1. Kinetic modeling and adsorption parameters of CPPCR toward Pb(II), Cd(II) and Cr(III)

Metal	Lagergren		Ho & McKay		Santosa	
	R^2	k (min^{-1})	R^2	k ($\text{g mg}^{-1} \text{min}^{-1}$)	R^2	k (min^{-1})
Pb	0.6187	0.012	0.9974	0.135	0.4596	0.003
Cd	0.4369	0.007	0.9977	1.423	0.6842	0.017
Cr	0.6256	0.013	0.9244	0.016	0.4361	0.001

for Cd(II) (2.28 mg g^{-1}) was the lowest compared to Pb(II) (4.63 mg g^{-1}) and Cr(III) (3.70 mg g^{-1}).

Adsorption Isotherms Behavior The adsorption isotherm behavior of CPPCR for Pb(II), Cd(II) and Cr(III) metals

was determined by applying the Langmuir, Freundlich and Temkin models. The linear plot of the adsorption isotherm of CPPCR is presented in Figure 10 (Langmuir), Figure 11 (Freundlich) and Figure 12 (Temkin model). On the basis of correlation coefficient the adsorption

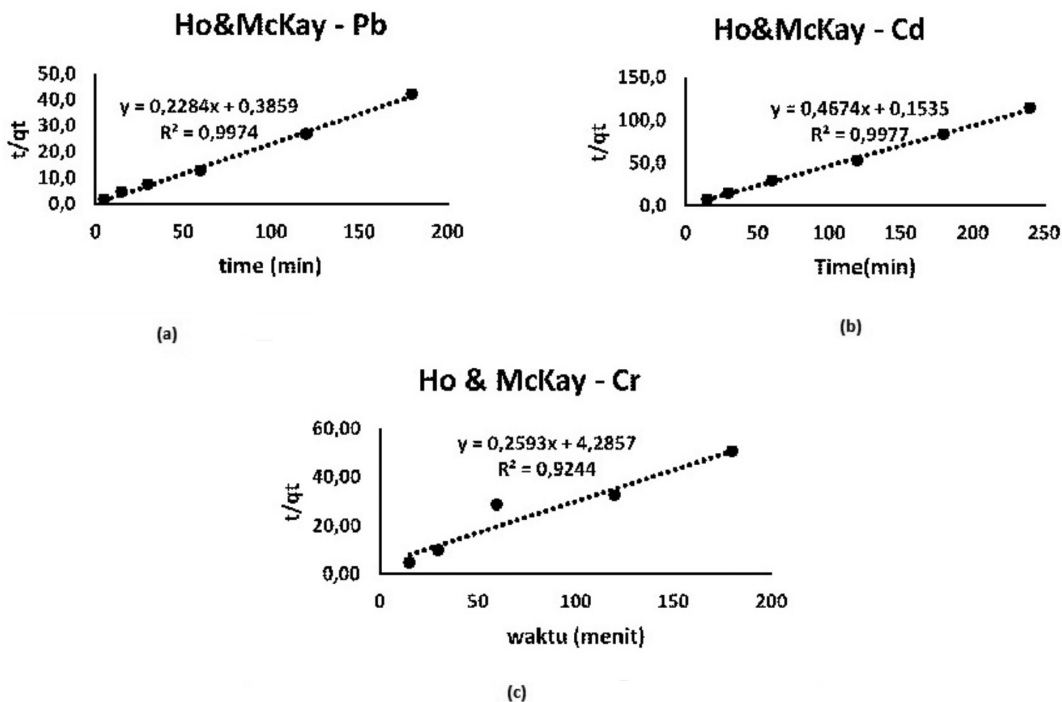


FIGURE 9. Ho-MacKay pseudo 2nd order plots for the adsorption of (a) Pb(II) and (b) Cd(II) and (c) Cr(III) by CPPCR in aqueous solution

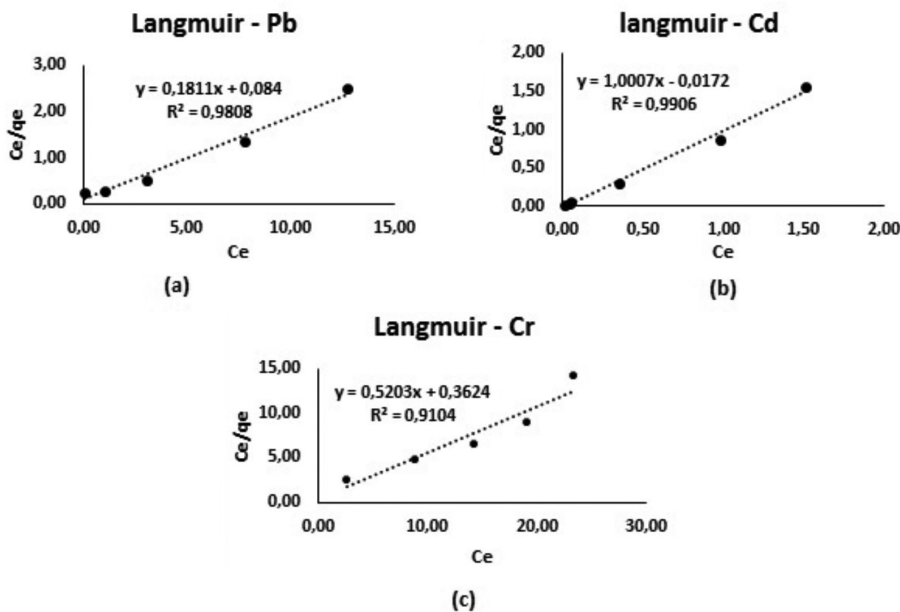


FIGURE 10. Langmuir plots for the adsorption of (a) Pb(II), (b) Cd(II) and (c) Cr(III) by CPPCR

isotherm of CPPCR against Pb(II), Cd(II) and Cr(III) preferred Langmuir models with the highest R^2 (> 0.90). Therefore, it can be assumed that the adsorption process occurs on the monolayer system or model (de Namor et al. 2011; Kim et al. 2015). The Langmuir, Freundlich and Temkin equation parameters of the CPPCR against Pb(II), Cd(II) and Cr(III) are also presented in Table 2.

The separation factor (R_L) can be calculated from the Langmuir equation, $R_L = 1 / (1 + K_L C_0)$ where C_0 (mg/L)

is the initial metal ions concentration and K_L (L/mg) is the adsorption effectiveness. The fact that R_L for the Pb(II), Cd(II), Cr(III) metals were 0.190; 0.017 and 0.065, respectively, indicating that the determining step of isotherms rate for the adsorption onto CPPCR was favorable. In general, the adsorption is favorable when $0 < R_L < 1$ and the lower value of R_L the more favorable adsorption will be.

Thermodynamic parameter of Gibbs free energy (ΔG) for the retention of adsorbate on adsorbent was determined

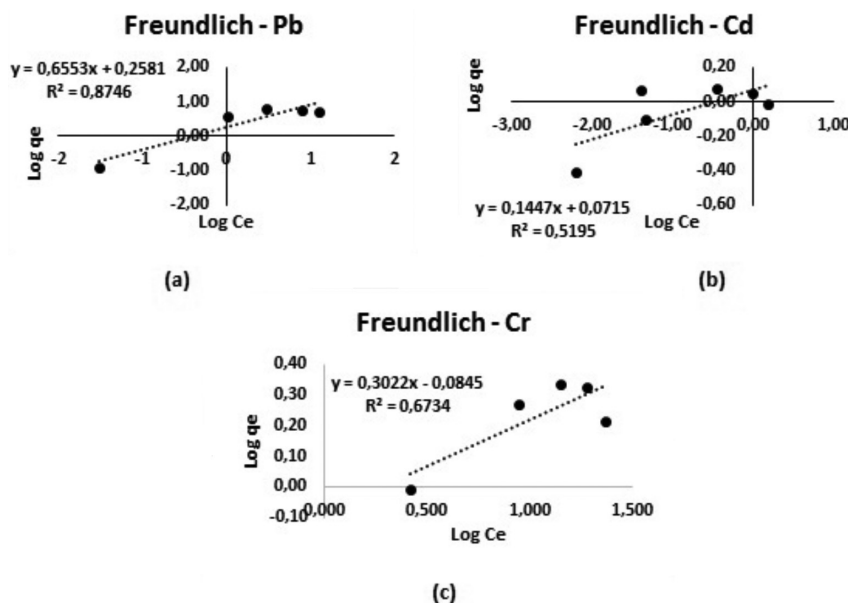


FIGURE 11. Freundlich plots for the adsorption of (a) Pb(II), (b) Cd(II), and (c) Cr(III) by CPPCR

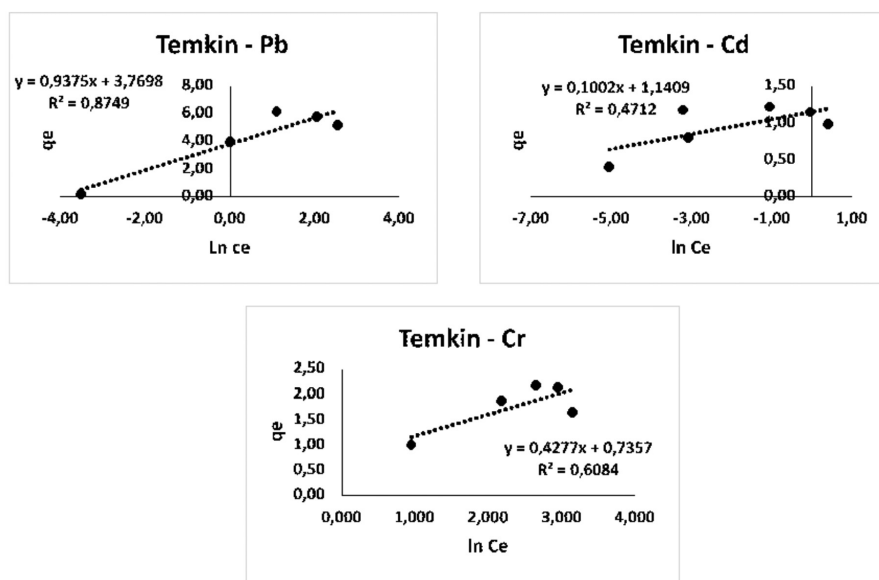


FIGURE 12. Temkin plots for the adsorption of (a) Pb(II), (b) Cd(II), and (c) Cr(III) by CPPCR

TABLE 2. Adsorption isotherms parameters based on Langmuir, Freundlich and Temkin

Metal	Langmuir					Freundlich			Temkin		
	R ²	q _m (mg/g)	K _L (L.mg ⁻¹)	R _L	E (kJ.mol ⁻¹)	R ²	K _F (mg.g ⁻¹)	n	R ²	b _r (L.g ⁻¹)	A _r
Pb	0.9808	5.52	2.16	0.190	-32.45	0.8746	1.81	1.53	0.8749	2664.48	55.76
Cd	0.9906	1.00	58.18	0.017	-39.13	0.5195	1.18	6.91	0.4712	24892.22	88.099
Cr	0.9910	1.92	1.44	0.065	-27.99	0.5734	1.22	3.31	0.6084	5831.66	1.22

to evaluate the feasibility of the adsorption process with the aid of equation $\Delta G = -RT \ln K$, where R is the ideal gas constant ($8.314 \text{ J K}^{-1} \text{ mol}^{-1}$), T is the absolute temperature (K) and K is the adsorption equilibrium constant (L.mol^{-1}).

The Gibbs free energy for adsorption based on the Langmuir isotherm model is presented in Table 2. The negative calculated ΔG values obtained for Pb(II), Cd(II) and Cr(III) indicate the adsorption were spontaneous. Both

the equilibrium constants (K_L) and Gibbs free energy of the adsorption follow the order of $\text{Cd(II)} > \text{Pb(II)} > \text{Cr(III)}$. The Gibbs free energies were also found to be higher than $20 \text{ kJ}\cdot\text{mol}^{-1}$ (27.99; 32.45; and $39.13 \text{ kJ}\cdot\text{mol}^{-1}$) indicating the adsorption involves chemisorption as an important step.

The reported ΔG values for C-4-methoxyphenylcalix[4]resorcinarene (CMPCR) adsorption for Pb(II) and Cr(III) adsorption were -29.576 and $-23.332 \text{ kJ}\cdot\text{mol}^{-1}$, respectively (Jumina et al. 2007). De Namor et al. (2001) has synthesized calix(4)arene ketone derivatives (5,11,17,23-tetra-tert-butyl-25,26,27,28-tetra(benzoyl)methoxycalix(4)) and investigated its interaction with alkali metal. The Gibbs energies of the calix(4)arene ketone derivatives in various solvents at 298.15 K was found within the range of $15\text{--}20 \text{ kJ}\cdot\text{mol}^{-1}$. In the present work, CPPCR has Gibbs free energy for Cd(II), Pb(II), and Cr(III) of 39.13; 32.45 and $27.99 \text{ kJ}\cdot\text{mol}^{-1}$, respectively, which are much higher than that of the previous calix. This may be due to the active sites such as carbonyl ($\text{C}=\text{O}$), ether ($-\text{O}-$) and hydroxyl (OH) which can interact with Pb(II), Cd(II) and Cr(III) (Utomo et al. 2009). On the other hand, CMPCR has only hydroxyl active group and the calix(4)arene ketone derivatives have two active groups of carbonyl and ether.

Effect of pH The initial pH of the solution can affect the speciation of the metal ions in aqueous solution, surface charge and dissociation or association of the functional group on the active sites of the adsorbent surface. The effect of pH on the adsorption capacity of CPPCR was studied in the pH range 2.0–8.0. Figure 13 shows an unusual dependency pattern of Pb(II) adsorption which gave maximum adsorption capacity at pH 4 and 6. This result is similar to the adsorption of Pb(II) on polypropylcalix[4]arene which has 2 optimum pH at 2.0 and 5.0, while for Cr(III) was at pH 5.0 (Akpomie & Dawodu 2014). On the other hand, the optimum pH of CPPCR adsorption against Cd(II) only showed one optimum pH at 6.0 and Cr(III) around 4.5.

At lower pH, the phenolic and carbonyls group may get protonated and the metal exists as $[\text{M}(\text{H}_2\text{O})_x]^{n+}$ cations.

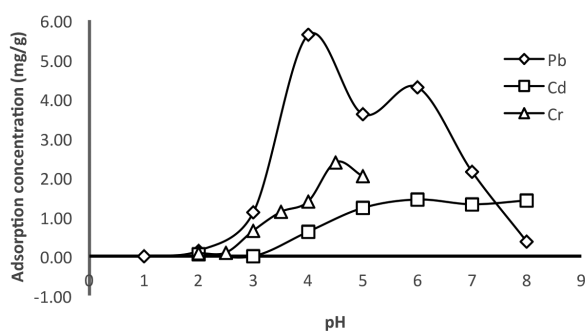


FIGURE 13. Effect of pH on the adsorption of Pb(II), Cd(II) and Cr(III) by CPPCR

Moreover, at higher concentration of H^+ ions present in the solution will initiate the competition between the metal ions and the protons to the adsorbent's active sites (Bell et al. 1998). Since both adsorbate and adsorbent have a similar charge, the electrostatic repulsive force will not allow the effective binding and adsorption to occur. The reduction of repulsive force as pH increases will increase the adsorption. The increase of adsorption uptake as pH increases was observed for both metals Pb(II) and Cr(III) with the optimum pH at 4 and 4.5, while the optimum capacity for Cd(II) was higher at pH 6.0. As the pH is increased, the metal ions can undergo hydrolysis to form several species in equilibrium. Lead is known to form several species such as PbOH^+ , $\text{Pb}(\text{OH})_2$, $\text{Pb}(\text{OH})_3^-$, $\text{Pb}_2(\text{OH})_3^+$, $\text{Pb}_3(\text{OH})_4^{2+}$, $\text{Pb}_4(\text{OH})_4^{4+}$ and $\text{Pb}_6(\text{OH})_8^{4+}$ (Mulya et al. 2014). The anionic species will certainly bind with protonated calix and caused the increase of the adsorption. It is known that when the pH is greater than 6.7, the neutral $\text{Pb}(\text{OH})_2$ (if it is produced) will be precipitated and consequently reduce the adsorption. In the alkaline environment, the phenolic groups of the calix will be deprotonated and the active sites will be more negative. In this condition, if there are still many hydrolyzed lead species with a positively charged, it will bind to calix and give the second maximum adsorption. In the case of C-4-hydroxyphenylcalix[4]resorcinarene, it has only one maximum adsorption condition was observed at pH 5.6.

Based on the speciation of lead and cadmium metals, Pb^{2+} is present at pH below 7 and Cd^{2+} species at below 9. In this work, the optimum pH of CPPCR was achieved at pH 4.0 and 6.0 for the adsorption of Pb(II) and Cd(II), respectively. Thus, it can be concluded that the removal of lead and cadmium was largely due to adsorption and not by precipitation. This fact is consistent with the work conducted by Das and Jana (2006) on the adsorption of Pb, Cu, and Cd on manganese nodule leached residues.

Figure 14 shows the percentage removal order of the metal ions by CPPCR is in the order of $\text{Cd(II)} > \text{Pb(II)} > \text{Cr(III)}$. The lowest % removal of Cr(III) was due to the presence of Cr^{3+} species in an acidic solution (pH less than 2) which expected to compete with the protonation (H^+). The maximum adsorption of Cr(III) onto CPPCR was observed to occur at pH 4.5, although the Cr^{3+} species compete with the formation of $\text{Cr}(\text{OH})^{2+}$, $\text{Cr}(\text{OH})_2^+$ dan $\text{Cr}_3(\text{OH})_4^{5+}$. Ramos et al. (1995) has investigated the adsorption of activated carbon for Cr(III) which showed an effective adsorption above pH 2.0 and below pH 6.4 with optimum pH at pH 5. This range of pH gave a profile that there were no Cr(III) adsorbed at pH 2 while at pH 6.4 the precipitation as $\text{Cr}(\text{OH})_3$ was formed and it was not adsorbed by the activated carbon matrix.

Effect of Initial Metal Ion Concentrations The adsorption capacity ($\text{mg}\cdot\text{g}^{-1}$) is the maximum adsorption of metal per g adsorbent. The initial concentration of the adsorbate also influences the adsorption capacity in a fixed amount of adsorbent. Figure 15 shows the varying maximum

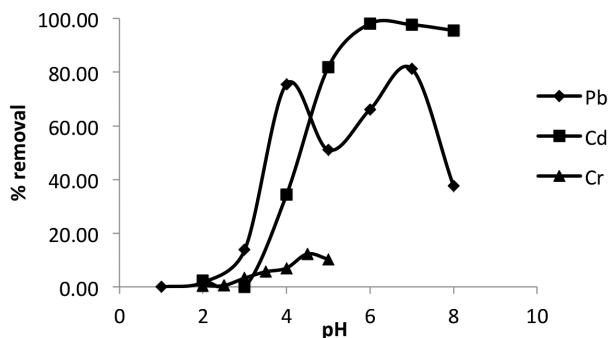


FIGURE 14. Effect of pH on %removal of Pb(II), Cd(II) and Cr(III) by CPPCR

capacity of 0.01 g CPPCR to Pb(II), Cd(II) and Cr(III) while the initial concentration of the metal ions was varied between 0.5 and 25 mg.L⁻¹. The maximum capacity of Pb(II) reached its highest amount when the initial concentration was 10 mgL⁻¹ while for Cd(II) and Cr(III) were 2 and 15 mgL⁻¹, respectively. Above these values, the adsorption capacity begins to decrease. Generally, increasing of adsorption capacity of adsorbent with the increase of metal ion concentrations could be due to the metal ions interaction with adsorbent that could overcome the resistance of the mass transfer of metal ions between the aqueous phase and the adsorbent (Arshadi et al. 2014; Bell et al. 1998). Meanwhile, the decreasing of the adsorption capacity is due to the declining of active sites vacancies that might become saturated after they reach some concentration (Ramos et al. 1995).

Morphology of Adsorbent Unlike carbon or carbohydrate which has surface with pores, the calix-based adsorbent is solid granule with irregular shape with the size between 250 and 100 mesh as shown by Scanning Electron Microscopy (SEM) micrograph in Figure 16. The surface of CPPCR before and after adsorption process against Pb(II) was observed. The figure shows that CPPCR

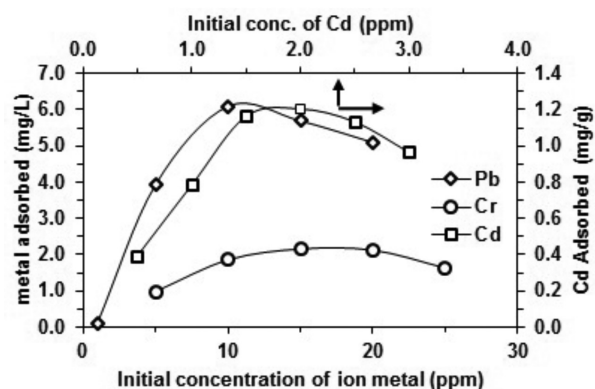
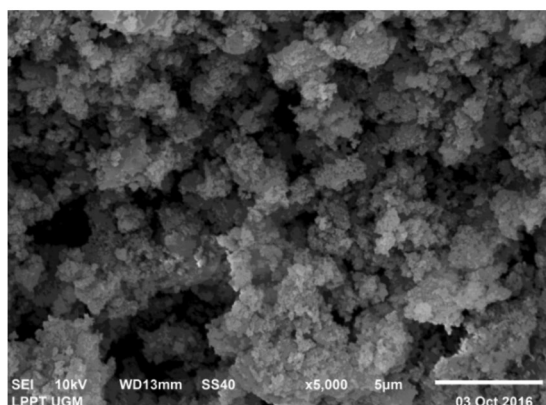


FIGURE 15. Effect of initial metal ion concentration on adsorption of Pb(II), Cd(II), and Cr(III) onto CPPCR (adsorbent dose 0.01 g, pH 4.0 for Pb(II), 6.0 for Cd(II) and 4.5 for Cr(III))

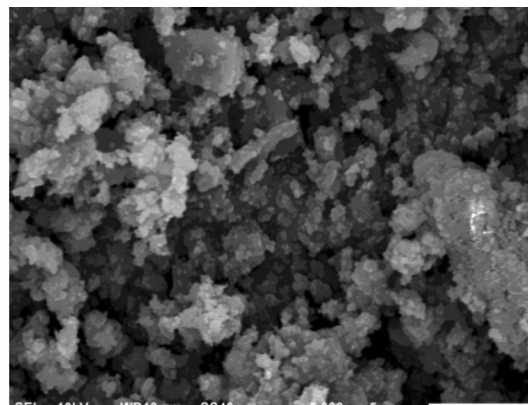
was sparsely porous and there was little change in the morphology of the calix except that the irregular solid became less agglomerate after the adsorption. Moreover, SEM analysis indicated that structure of C-4-phenacyloxy phenyl calix[4]resorcinarene was amorphous.

CONCLUSION

C-4-phenacyloxy phenyl calix[4]resorcinarene (CPPCR) with more functional groups present compare to its previously reported calix also showed good adsorption capacity against Pb(II), Cd(II) and Cr(III). The adsorption kinetics followed Ho's pseudo-second-order kinetic model and the adsorption isotherm adopted Langmuir isotherm model. The adsorption Gibbs free energy of Cd(II), Pb(II) and Cr(III) onto CPPCR are 38.13, 32.45 and 27.29 kJ mol⁻¹, respectively. Meanwhile, the adsorption capacity of CPPCR for Pb(II), Cd(II) and Cr(III) are 4.63, 2.28 and 3.70 mg g⁻¹, respectively. Although the maximum capacity for calix and other synthetic compounds are lower than the carbons their potential to remove low level metal content in solution is very promising.



(a) CPPCR before adsorption



(b) CPPCR after adsorption of Pb

FIGURE 16. Morphology of CPPCR before and after adsorption of Pb(II) at 5000 magnification

ACKNOWLEDGEMENTS

The authors are grateful to the Ministry of Research, Technology and Higher Education of the Republic of Indonesia through the Research Grant Disertasi Doktor 2016 and Postgraduate Scholarship for the financial support. Our appreciation is also to Prof. Dr. Roslan Abd-Shukor of School of Applied Physics, UKM for reading through the manuscript.

REFERENCES

- Abbas, M., Kaddour, S. & Trari, M. 2014. Kinetic and equilibrium studies of cobalt adsorption on apricot stone activated carbon. *Journal of Industrial and Engineering Chemistry* 20(3): 745-751.
- Akkus, G.U., Memon, S., Sezgin, M. & Yilmaz, M. 2009. Synthesis of calix(aza)crown and its oligomeric analogue for the extraction of selected metal cations and dichromate anions. *Clean* 37(2): 109-114.
- Akpmie, K.G. & Dawodu, F.A. 2014. Efficient abstraction of nickel(II) and manganese(II) ions from solution onto an alkaline modified montmorillonite. *Journal of Taibah University for Science* 8(4): 343-356.
- Arshadi, M., Amiri, M.J. & Mousavi, S. 2014. Kinetic, equilibrium and thermodynamic investigation of Ni(II), Cd(II), Cu(II) and Co(II) adsorption on barley straw ash. *Water Resources and Industry* 6: 1-17.
- Babel, S. & Kurniawan, T.A. 2003. Low-cost adsorbents for heavy metals uptake from contaminated water: A review. *Journal of Hazardous Materials* B97: 219-243.
- Barnhart, J. 1997. Occurrences, uses, and properties of chromium. *Regulatory Toxicology and Pharmacology* 26: S3-S7.
- Bell, S.E.J., Browne, J.K., McKee, V., McKervey, M.A., Malone, J.F., O'Leary, M., Walker, A., Arnaud-Neu, F., Boulangeot, O., Mauprivez, O. & Schwing-Weill, M.J. 1998. Cation complexation by chemically modified calixarenes. 11. Complexation and extraction of alkali cations by calix[5]- and -[6]arene ketones. Crystal and molecular structures of calix[5]arene ketones and Na⁺ and Rb⁺ complexes. *Journal of Organic Chemistry* 63: 489-501.
- Benavente, M., Moreno, L. & Martinez, J. 2011. Sorption of heavy metals from gold mining wastewater using chitosan. *Journal of the Taiwan Institute of Chemical Engineers* 42(6): 976-988.
- Bhattacharyya, K.G. & Gupta, S.S. 2008. Adsorption of a few heavy metals on natural and modified kaolinite and montmorillonite: A review. *Advances in Colloid and Interface Science* 140: 114-131.
- Das, N. & Jana, R.K. 2006. Adsorption of some bivalent heavy metal ions from aqueous solutions by manganese nodule leached residues. *Journal of Colloid and Interface Science* 293(2): 253-262.
- de Namor, A.F.D., Kowalska, D., Castellano, E.E., Piro, O.E., Velarde, F.J.S. & Salas, J.V. 2001. Lower rim calix(4) arene ketone derivatives and their interaction with alkali metal cations. Structural and thermodynamic (solution and complexation) characterisation of the tetraphenyl ketone derivative and its sodium complex. *Physical Chemistry Chemical Physics* 3: 4010-4021.
- Flora, G., Gupta, D. & Tiwari, A. 2012. Toxicity of lead: A review with recent updates. *Interdisciplinary Toxicology* 5(2): 47-58.
- Gunatilake, S.K. 2015. Methods of removing heavy metals from industrial wastewater. *Journal of Multidisciplinary Engineering Science Studies* 1(1): 12-18.
- Gupta, S.S. & Bhattacharyya, K.G. 2009. Treatment of water contaminated with Pb(II) and Cd(II) by adsorption on kaolinite, montmorillonite and their acid-activated forms. *Indian Journal of Chemical Technology* 16: 457-470.
- Gutsche, C.D. 2008. *Calixarenes: An Introduction*. 2nd ed. Monographs in Supramolecular Chemistry. The Royal Society of Chemistry, Cambridge-UK.
- Jaishankar, M., Tseten, T., Anbalagan, N., Mathew, B.B. & Beeregowda, K.N. 2014. Toxicity, mechanism and health effects of some heavy metals. *Interdisciplinary Toxicology* 7(2): 60-72.
- Joshi, J. & Sahu, O. 2014. Adsorption of heavy metals by biomass. *Journal of Applied & Environmental Microbiology* 2(1): 23-27.
- Jumina, Sarjono, R.E., Siswanta, D., Santosa, S.J. & Ohto, K. 2011. Adsorption characteristics of Pb(II) and Cr(III) onto C-methylcalix[4]resorcinarene. *Journal of the Korean Chemical Society* 55(3): 454-462.
- Jumina, Sarjono, R.E., Paramitha, B., Hendaryani, I. & Siswanta, D. 2007. Adsorption characteristics of Pb(II) and Cr(III) onto C-4-methoxyphenylcalix[4]resorcinarene in batch and fixed bed column system. *Journal of the Chinese Chemical Society* 54: 1167-1178.
- Kim, J.Y., Morisada, S., Kawakita, H., Ohto, K. & Kim, Y. 2015. Relationship between chemical structure and extraction efficiency toward palladium with ketonic derivatives of p-tert-octylcalix[4]arene in nitric acid media. *Journal of Inclusion Phenomena and Macrocyclic Chemistry* 82(1): 25-32.
- Kunsagi-Mate, S., Szabo, K., Lemli, B., Bitter, I., Nagy, G. & Kollar, L. 2005. Host-guest interaction between water-soluble calix[6]arene hexasulfonate and p-nitrophenol. *Thermochimica Acta* 425(1-2): 121-126.
- Li, X., Wang, Z., Li, Q., Ma, J. & Zhu, M. 2015. Preparation, characterization, and application of mesoporous silica-grafted graphene oxide for highly selective lead adsorption. *Chemical Engineering Journal* 273: 630-637.
- Ming, C., Ting, S., Wei, F. & Guowang, D. 2011. Study on adsorption and desorption properties of the starch grafted p-tert-butyl-calix[n]-arene for butyl Rhodamine B solution. *Journal of Hazardous Materials* 185: 914-921.
- Mouni, L., Merabet, D., Bouzaza, A. & Belkhir, I. 2011. Adsorption of Pb(II) from aqueous solution using activated carbon developed from apricot stone. *Desalination* 276(1-3): 148-153.
- Mulya, P.W., Jumina, J., Siswanta, D. & Ngurah, B.I.G.M. 2014. *Advanced Materials Research* 1043: 129-132.
- Mututuvvari, T.M. 2014. Supramolecular biopolymeric composite materials: Green synthesis, characterization, and applications. Dissertation. Marquette University, Wilwaukee, Wisconsin (Unpublished).
- Peng, W., Li, H., Liu, Y. & Song, S. 2017. A review on heavy metal ions adsorption from water by graphene oxide and its composites. *Journal of Molecular Liquids* 230: 496-504.
- Ramos, R.L., Rubio, L.F., Coronado, R.M.G. & Barron, J.M. 1995. Adsorption of trivalent chromium from aqueous solutions onto activated carbon. *Journal of Chemical Technology and Biotechnology* 62: 64-67.
- Rastuti, U., Siswanta, D. & Jumina. 2016. Synthesis and characterization of 4-Phenacyloxy benzaldehyde derivatives. *Oriental Journal of Chemistry* 32(5): 2451-2458.

- Reddy, N.S. & Rao, K.S.V.K. 2016. Polymeric hydrogels: Recent advance in toxic metal ion removal and anticancer drug delivery applications. *Indian Journal of Advances in Chemical Science* 4(2): 214-234.
- Sajab, M.S., Chia, C.H., Zakaria, S. & Sillanpää, M. 2017. Adsorption of heavy metal ions on surface of functionalized oil palm empty fruit bunch fibers: Single and binary system. *Sains Malaysiana* 46(1): 157-165.
- Sajab, M.S., Chia, C.H., Zakaria, S. & Khiew, P.S. 2013. Cationic and anionic modifications of oil palm empty fruit bunch fibers for the removal of dyes from aqueous solutions. *Bioresource Technology* 128: 571-577.
- Satarug, S., Baker, J.R., Urbenjapol, S., Haswell-Elkins, M., Reilly, P.E.B., Williams, D.J. & Moore, M.R. 2003. A global perspective on cadmium pollution and toxicity in non-occupationally exposed population. *Toxicology Letters* 137: 65-83.
- Schneider, I.A.H., Rubio, J. & Smith, R.W. 2001. Biosorption of metal onto plant biomass: Exchange adsorption or surface precipitation. *International Journal of Mineral Processing* 62(1-4): 111-120.
- Shariffard, H., Nabavinia, M. & Soleimani, M. 2016. Evaluation of adsorption efficiency of activated carbon/chitosan composite for removal of Cr(VI) and Cd(II) from single and bi-solute solution. *Advances in Environmental Technology* 4: 215-227.
- Sitko, R., Turek, E., Zawisza, B., Malicka, E., Talik, E., Heimann, J., Gagor, A., Feist, B. & Wrzalik, R. 2013. Adsorption of divalent metal ions from aqueous solution using graphene oxide. *Dalton Transactions* 42(16): 5682-5689.
- Tran, C.D., Prosenč, F., Franko, M. & Benzi, G. 2016. One-pot synthesis of biocompatible silver nanoparticle composites from cellulose and keratin: Characterization and antimicrobial activity. *ACS Applied Materials & Interfaces* 8(50): 34791-34801.
- Trawneh, S.A. 2015. Studies on adsorption removal of some heavy metals ions by calix[4]resorcine. *Jordan Journal of Earth and Environmental Sciences* 7(1): 1-9.
- Utomo, S.B., Jumina & Wahyuningsih, T.D. 2009. The adsorption of Pb(II) and Cr(III) by polypropylcalix[4]arene polymer. *Indonesian Journal of Chemistry* 9(3): 437-444.
- Zhang, Y., Zheng, R., Zhao, J., Ma, F., Zhang, Y. & Meng, Q. 2014. Characterization of -treated rice husk adsorbent and adsorption of copper (II) from aqueous solution. *BioMed Research International* 2014: Article ID. 496878.

Undri Rastuti, Dwi Siswanta, Wisnu Pambudi,
Beta Achromi Nurohmah & Jumina*
Department of Chemistry
Faculty of Mathematics and Natural Sciences
Universitas Gadjah Mada, Sekip Utara Bulaksumur
Yogyakarta 55281
Indonesia

Undri Rastuti
Department of Chemistry
Faculty of Mathematics and Natural Sciences
Universitas Jenderal Soedirman, Jl. dr. Soeparno Karangwangkal
Purwokerto 53122
Indonesia

Bohari M. Yamin
Faculty of Science and Technology
Universiti Sains Islam Malaysia
71800 Nilai, Negeri Sembilan Darul Khusus
Malaysia

*Corresponding author; email: jumina@ugm.ac.id

Received: 23 November 2017
Accepted: 6 January 2018